Journal of Applied Sciences

ISSN 1812-5654

science alert

ANSInet
an open access publisher
http://ansinet.com

Journal of Applied Sciences 15 (8): 1059-1072, 2015
ISSN 1812-5654

RESEARCH ARTICLE OPEN ACCESS

DOI: 10.3923/jas.2015.1059.1072

Development of a Hybrid Ultrasonic and Optical Sensing for Precision Linear Displacement Measurement

Abdallah Alsayed, Muhammed Razif Mahadi, Aimrun Waykok and Wan Ishak B. Wan Ismail
Department of Biological and Agricultural Engineering, Faculty of Engineering, Universiti Putra Malaysia, UPM Serdang, Selangor, 43400, Malaysia

ARTICLE INFO
Article History:
Received: May 18, 2015
Accepted: August 06, 2015

Corresponding Author:
Abdallah Alsayed
Department of Biological and Agricultural Engineering,
Faculty of Engineering,
Universiti Putra Malaysia,
UPM Serdang, Selangor, 43400,
Malaysia

ABSTRACT
This study presents a proposed technique for displacement measurement in linear horizontal motion. The measurement system consists of a lines can sensor with built in illumination system, grating scale and an ultrasonic sensor. Once, the linescan transducer scans the grating scale optically, the displacement of the transducer is measured based on pixel shifting method. Additionally, the role of the ultrasonic sensor is to add the reference position for the linescan transducer and the current position in case of missing the position. The linescan transducer design includes; the illumination source and the division of the grating scale. The accuracy of the measurements is compared to white and infrared lights. After that, the comparison is built based on three scale divisions which are 0.5, 1 and 2 mm. Finally, the accuracy also is compared to different travelling ranges of motion. The displacement measurements of the proposed transducer is evaluated comparatively to Optiv Light Measurement (OLM) device.

Key words: Displacement, linescan, illumination, ultrasonic sensor

INTRODUCTION

The optical sensor has photo detector, which is sensitive to the light. The light interruption on the photo detector generates a pulse (Haus, 2010; Nagai *et al*., 2013). In optical sensor, the pulse is the core of displacement sensing which represents as a function of the incident light, as in:

$$\text{Output voltage} = K \times \text{Light intensity} \times \text{Integration time} \quad (1)$$

where, K is a constant and the integration time is the period of photodiode's charging time (Cano-Garcia *et al*., 2007). One pulse is defined as two successive events of rising and falling edges (Feng, 1996; Alsayed and Mahadi, 2014). In linear grating scale, there is a number of transparent and non-transparent slots, which is called monochrome stripe. If the grating scale has N number of transparent slots, also the non-transparent and transparent slots have the same width, the full distance of the grating is 2 N. The inverse of the distance represents the resolution of the sensor, which is 1/2 N. Additionally, the error of measurements is ±1/2 N (Kajima and Minoshima, 2014).

The single point optical sensor gives two different phases while scanning (Viollet and Franceschini, 2010). It can be replaced with a linescan sensor. The linescan sensor has a single row array of photo detectors. These photo detectors have greater capacity that increase the capability of scanning. The feature of using linescan sensor is to track the displacement within the width of photo detector or within width of several photo detectors in a cut view scope (Corradi *et al*., 2008). This study presents a proposed technique for displacement measurement in linear horizontal motion.

MATERIALS AND METHODS

Linescan module design: The design concept of the transducer would resemble a camera, with a linescan chip (TSL1401 CL) as the sensing component (Fig. 1b). The chip was TSL1401CL, consisted of a single row array of 128 photodiodes. The dimension of each photodiode is 63.5 µm in height by 55.5 µm in width. The overall length of the array is 8.128 mm. Each photodiode constitutes a pixel; hence, there are 128 pixels within this chip. The linescan chip was sensitive to light, thus it was completely enclosed in order to prevent leakage of external illumination or otherwise it will jeopardize the accuracy of the measurement. The image of the

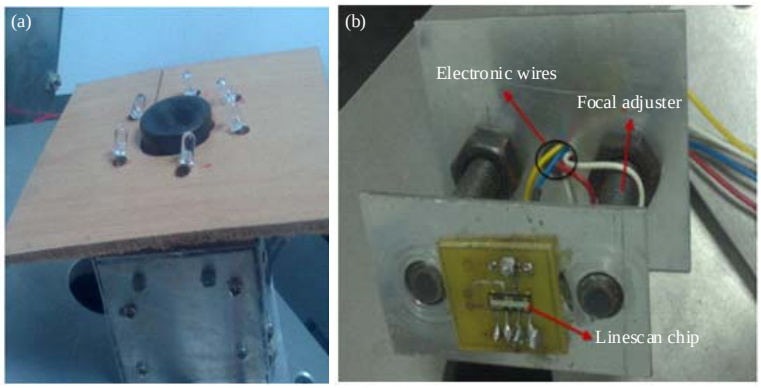

Fig. 1(a-b): (a) Outer components of the module and (b) Inner components of the module

measured object must be focused into the linescan array. Therefore, 8 mm CCTV camera lens was installed to the aperture of the transducer. On the array, the two dimensional image has two dimensions; the length and the height. However, the significant one was the length of the image because, it was in the same direction of the motion. Hence, the width was ignored.

Six infrared LEDs were added to be part of the transducer with the aim of providing enough brightness to light up the focus zone (Fig. 1a). Two sets of three LEDs are put around the aperture. Having arranged the LEDs this way allows the brightness on the focused area to be spread rather than having a concentrated intensity converging at the center. The ring arrangement gives the optimum brightness for zone area. For a single LED, the irradiance distribution (W m^{-2}) is given by:

$$E(r, \theta) = E_o(r)\cos^m \theta \quad (2)$$

Where:

$E_o(r)$ = The irradiance at distance r from the LED
θ = The view angle of the LED
m = A number

However, in term of Cartesian coordinates (x, y, z), if the LED is positioned at point (x_o, y_o), the irradiance over point (x, y) at distance z can be given by:

$$E(x,y,z) = \frac{z^m I_{LED}}{[(x - x_o)^2 + (y - y_o)^2 + z^2]^{(m+2)/2}} \quad (3)$$

where, I_{LED} is the LED intensity (W/s_r). Now, for six LEDs are arranged as, a ring around the aperture of the linescan module, the irradiance E(x, y, z) is given by:

$$E(x,y,z) = z^m \sum_{N=1}^{6} Ij[(x - r\cos(\frac{2\pi}{N}))^2 + (y - r\sin(\frac{2\pi}{N}))^2 + z^2]^{-(m+2)/2} \quad (4)$$

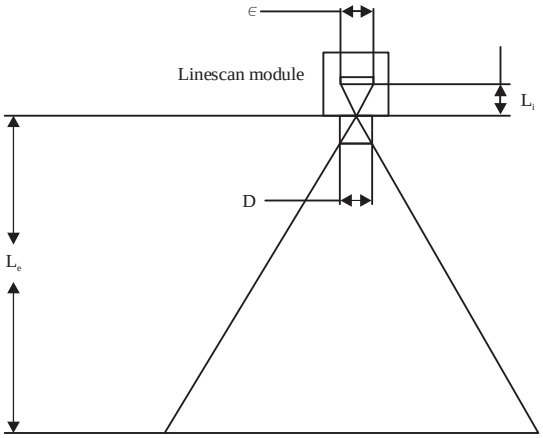

Fig. 2: Schematic diagram of optic system

Where:

r = The radius of the ring
N = The number of the LEDs in the ring (Lambert *et al*., 2011; Shi *et al*., 2014)

Based on Depth From Focus (DFF) method (Miwa *et al*., 2000), a relationship is established to measure the distance between the linescan module and the grating scale. The distance L_i between the pitch of array of linescan chip and the lens relies strongly on the focal length L_f and the distance L_e between the grating scale and the lens (Fig. 2). The relation between L_i, L_f and L_e us given by:

$$\frac{1}{L_f} = \frac{1}{L_i} + \frac{1}{L_e} \quad (5)$$

However, this equation can be used without determination the depth of field, which let us know the maximum distance between the front aperture of the module and the grating scale. In order to determine the depth of field, the pitch of the array of linescan chip and the diameter of the

lens are taken into the consideration. In Eq. 6, ∀ is the depth of field, is the pitch of array and D is the diameter of the lens:

$$\forall = \frac{\in L_e L_f D(L_e - L_f)}{L_f^2 D^2 - \in^2 (L_e - L_f)^2} \quad (6)$$

Relationship between image resolution, illumination and grating scale division: The displacement measurement based on linescan transducer has limitation with pixel resolution. If the linescan sensor has N of pixels and the width of the stripes in the view scope is W mm, the resolution of the sensor is given by:

$$Res = \frac{W}{N} (mm/pixel) \quad (7)$$

A smaller stripes width, a finer resolution can be achieved. But, there is a limitation, especially if the speed of movement is high. The image resolution relies on the design of the illumination and the division of grating scale. Once, the light is generated, the energy in the light of the LED travels in a straight line toward the grating scale. However, the grating scale is made of paper material, therefore around 65% of light will be reflected, if the color of the stripe is white and 30% of the light will be reflected if the color of the stripe is black (Gou *et al*., 2011). Since, the photodiode output is related to the amount of light intensity, two levels of high voltage and low voltage are the output based on the stripes color. In LED propagation, a single LED is not enough to cover the entire area of the view scope. Hence, the stripes image is not seen on the entire span of the sensor array. As in Zhu *et al*. (2011), a uniform illumination design was achieved using ring array of LEDs. A ring of 16 LEDs could light a surface, which had radius of 100 mm. In our case, a ring of six LEDs can illuminate the scale surface with radius of 30 mm (Protzman and Houser, 2006; Richard, 2007; Lee and Liu, 2012).

Not just the illumination is enough to generate sharp and clear stripes image; the significance of the image premises on form the square pulses without overlapping between rise and fall edges. To avoid overlapping, the distance between stripes edges have to be taken into consideration. The time between stripes and velocity of movement can determine the gap between the edges. In that, Eq. 8 illustrates this relation:

$$gp = V \times T \quad (8)$$

Where:
gp = The stripe width
V = The velocity of motion
T = The sample time of pulse

The purpose of this equation is to avoid anti-aliasing condition (Mahadi, 2011).

Hardware and Initialization: The core component of the transducer is a linescan chip, which was initialized by an Atmega Arduino board. The original chip was a surface mount type, which required an intermediary board for ease of manipulation. There are six essential pins that include Serial Inputs (SI), clock (CLK), Analog Output (AO), voltage source (V_{dd}) and two pins for ground (GND) (Fig. 3). The linescan chip was initialized by Arduino microcontroller and merely two bits from Arduino were needed to control it. The function of SI input is to begin a scan, while CLK input is to latch the SI and clock the pixels out. The time integration (T) was a delay time after every scan process in order to get the desired output voltage and the minimum delay time can be calculated using Eq. 9:

$$T(min) = (128\text{-}18) \times clock + 20\ \mu sec \quad (9)$$

In case of light, if the photodiodes sense the external light, the sensor output is low if and only if the SI input is low. However, if the photodiodes sense the light and SI input is high, the internal amplifiers start charging the capacitors depending on the intensity of light. Then, in order to discharge the capacitors to the output, CLK input has to be high. The output of the linescan sensor is the image of the grating scale in the view scope.

Displacement measurements based on pixel shifting method: In displacement sensing, a set of white and black stripes is considered the basis of traditional incremental encoders (Giniotis and Grattan, 2002). Assuming an object originally positioned on a black stripe and after that shifted several stripes forward, if the number of stripes traversed and their sizes are known, the displacement for that object can be tracked. Pixel shifting method enhances the resolution of displacement measurement by moving the object typically a pixel between old image and new image being captured.

Consider an image taking at to using linescan array sensor in the view scope (Fig. 4). There are four stripes of white and

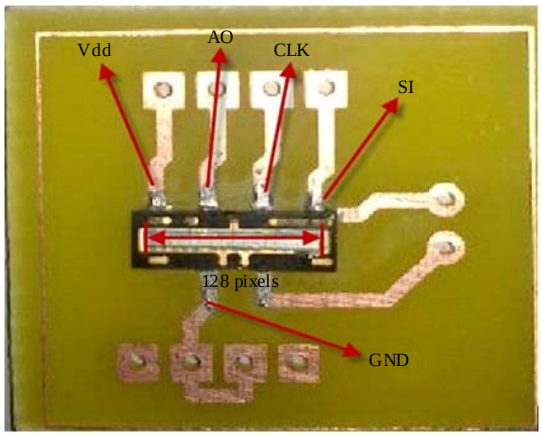

Fig. 3: Linescan sensor circuit

black. If the entire span of the sensor captures the view scope, 128 pixels provide the image voltages. The voltages of pixels ranged from 0 volt to V_{dd} volt based on intensity of light. Thresholding process provides two levels of binary bits, which are high and low. Using analog to digital port in a microcontroller device, the pixels voltage converted to 1 or 0 based on threshold value. As a result of thresholding process, 128 bits of 1 and 0 sec are assembled in a single row array. A binary bit 1 represents the white portion in the image, whereas 0 bit represents the black portion in the image. So, 128 bits are assembled in single array to be analyzed. Because of uniformity of stripes width, 128 pixels can be distributed over the entire width of view scope. In other words, one stripe has been captured by 32 pixels if we have 4 stripes in the view scope (Fig. 5).

Because, the designed grating scale is uniformed and the width of stripes is constant through the length of grating scale, two successive stripes of black and white are enough to be tracked. After thresholding process for two black and white stripes, Fig. 6 shows their image being captured. If the number of bits for black is 32 bits and it are captured by 32 pixels, every pixel has the value of one bit. Taking the first bit in black stripes as a reference position, the address of the first bit in black stripe image is array[1]. If the linescan module start moving and the next image as seen in Fig. 7, the new address of first bit in black stripe image is array[2]. In that, the module has moved one bit width in forward and the displacement is defined as the number of shifts (one shift) multiplied by the width of pixel (X = 63.5 μm). In general, if the module has moved one stripe, the pattern of bit shifting is shown in Fig. 8.

In Forward movement, the address of first bit is the reference for shifts counting. But, in backward movement, the address of last bit in white stripe is the reference for shifts

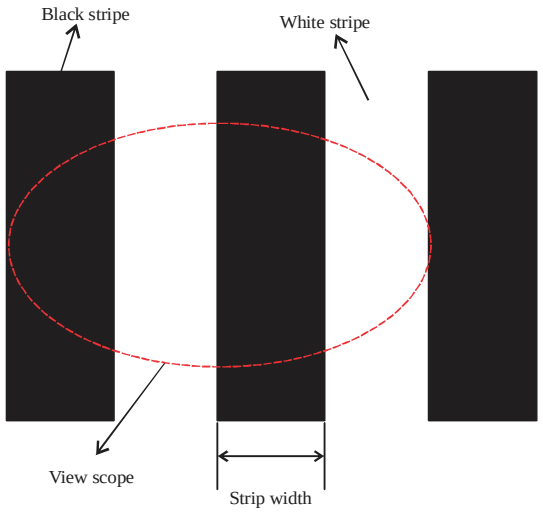

Fig. 4: View scope of linescan sensor

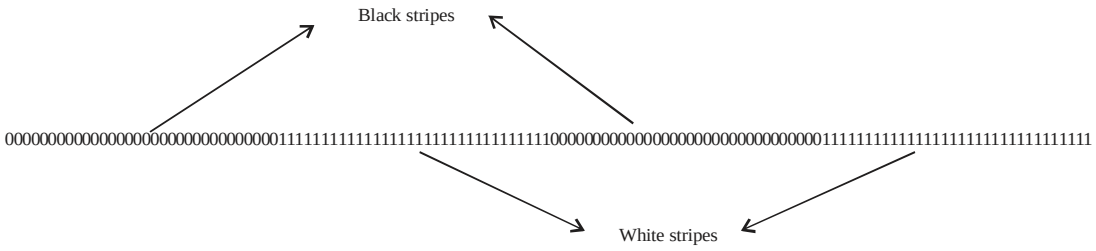

Fig. 5: Stripes image after thresholding process

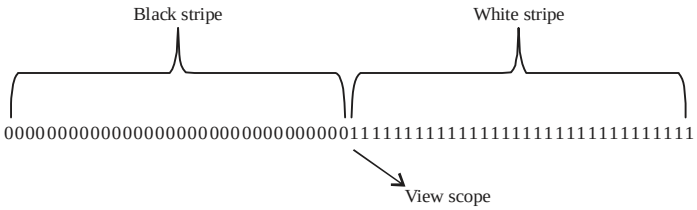

Fig. 6: Reference position

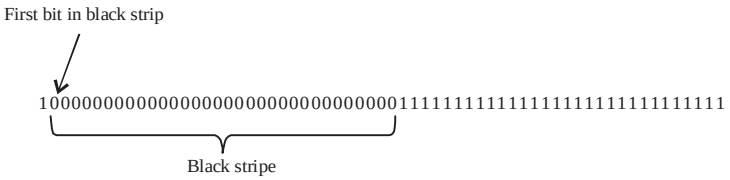

Fig. 7: One bit shifting as a result of 63.5 μm displacement by the module

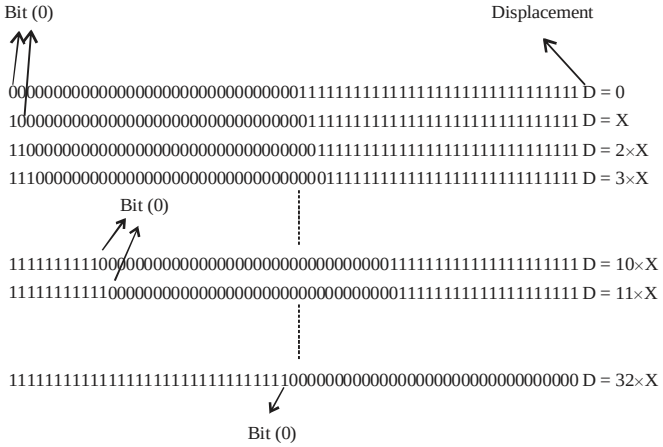

Fig. 8: Pattern of bit shifting after displacement of one stripe width

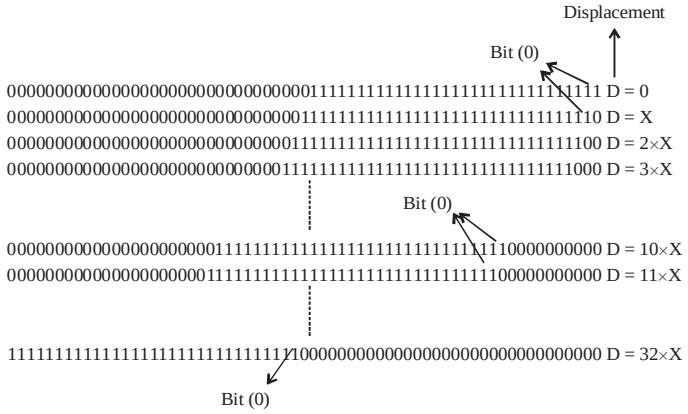

Fig. 9: Pattern of stripes image after motion in backward

counting. Similarly to forward movement, measure displacement is based on distance of shifting. Figure 9 shows the pixel shifting when the movement in backward.

If the module moves several stripes, the stripe counting has the same criteria with above two cases of motion. Overall, the equation for displacement measurements based on pixels shifting is derived as:

$$\text{Displacement} = (N_{p+}\text{-}N_{p-})\times\text{bit width} \quad (10)$$

Where:

N_{p+} = The number of pixel shifts in forward
N_{p-} = The number of pixel shift in backward
bit width = The width of the photodiode (63.5 μm) in the linescan sensor, if the image has the same width of sensor array

Integration of linescan module and ultrasonic sensor for displacement measurement: In the previous section, the displacement equation is prepared when the linescan module starts moving at the beginning of grating scale. On the other hand, if the linescan sensor start moving at unknown position on the grating scale, inaccurate measurement will be recorded. One of the best choice, to provide the system the initial position, is to add an ultrasonic sensor. The ultrasonic sensor provides the displacement in proximity. In addition, it is also

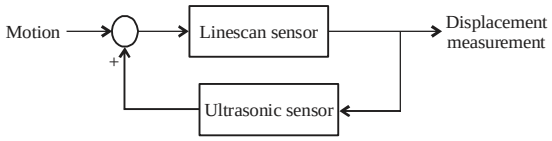

Fig. 10: An ultrasonic sensor is a feedback sensor for linescan sensor

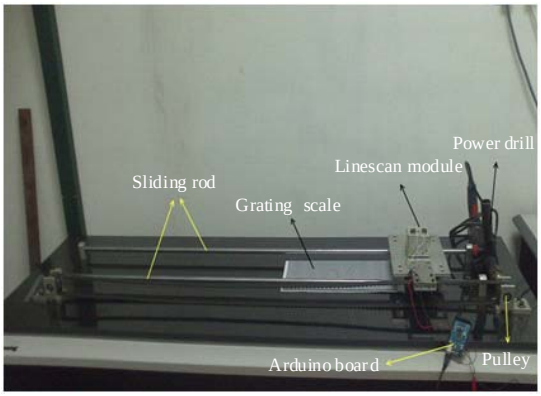

Fig. 11: Experimental set up

possible to make the ultrasonic sensor as a feedback sensor to the linescan sensor as in Fig. 10. When there is a significant difference between the reading of ultrasonic sensor and linescan sensor, the system reset the displacement reading, then the ultrasonic reading will be taken and start counting the stripes traversed based on linescan module. The displacement relation after adding an ultrasonic sensor is shown in Eq. 11:

$$\text{Displacement} = U_r+(N_{P+}-N_{P-})\times\text{bit width} \quad (11)$$

Where:
U_r = The reading of the ultrasonic sensor

RESULTS

Initialization the measurement system: The construction of the linear motion calibration system consists of the solid wood bed, transducer conveyor, grating scale, ultrasonic sensor and image captured module. The belt motion was executed by using power drill shaft which was connected to the pulley. The transducer output was connected to the analogue pins of Arduino microcontroller. As shown in Fig. 11, two sliding rods were designed to carry the transducer and to allow it to move freely in two direction. The module was fixed above the grating scale in such a way that the sensing element was perpendicular to the scale stripes. The aperture of the module was placed directly to the grating scale.

In order to run the transducer, the linescan sensor SI pin received an integration time with a duty cycle of 1 msec, while CLK pin received 128 of pulses which had duty cycle of

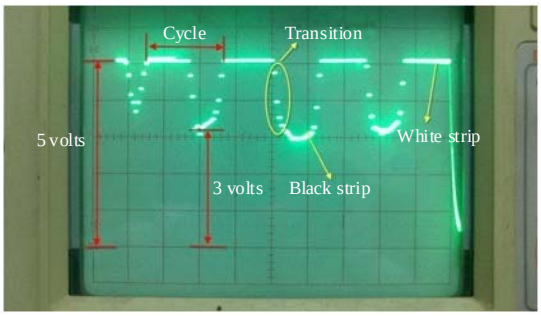

Fig. 12: Image of stripes as seen on the oscilloscope

20 µm. The linescan capturing was evaluated using a 2 mm grating scale. On the oscilloscope, the analog signal appears as in Fig. 12. The portions at 5 volts represented white stripes, whereas the portions measured at 3 volts represented the black stripes. The dots in between represented the gradual transition between the two phases. The image reflected on the sensor array was magnified by a factor of two. Therefore, there were eight stripes occupying the view scope, starting with a white stripe (on the left) and ending at another white stripe after four cycles (from the right). Since, the width of one stripe was 2 mm, the total width of the stripes in the view scope was 16 mm. On the linescan array, there were 128 pixels; ideally one stripe should fall on 16 pixels.

Using the serial monitor window in Arduino-Sketch the bits that represented the entire 128 pixels were read in real time (Fig. 13). In forward direction, the transitions between the stripes were shifted to the left with the value of the displacement. In contrast, the transitions were shifted to the right while the moving was in backward. Ideally, 16 bits should capture the size for one stripe. As seen in Fig. 13, the stripes bits number was closed to 16 at the center, while the number reduced significantly at the boundaries due to light convergence. Because of the light convergence around the central spot of the grating scale, the transitions at the center of the view scope were clearer than those at the boundaries. As mentioned, at least two stripes were required to track the displacement, so the clearest transitions should be targeted. Hence, for measurement of linear motion parameters, the signal from the central region should be considered.

Actual measurement of grating size based on OLM device: The OLM is a precision static measurement instrument (Fig. 14). It can measure the movement in lateral (y-axis) and longitudinal (x-axis) directions with a resolution of 1 µm and accuracy of 3 µm. The top lights of CCD camera were used, because the grating scales were printed on a paper, which meant that the background was solid and no lights can penetrate that.

Before measurements were conducted, three sets of scale divisions were prepared which were 1, 2 and 0.5 mm. As shown in Fig. 14, the scale, to be measured, should be placed on the movable part of the device, while the CCD camera

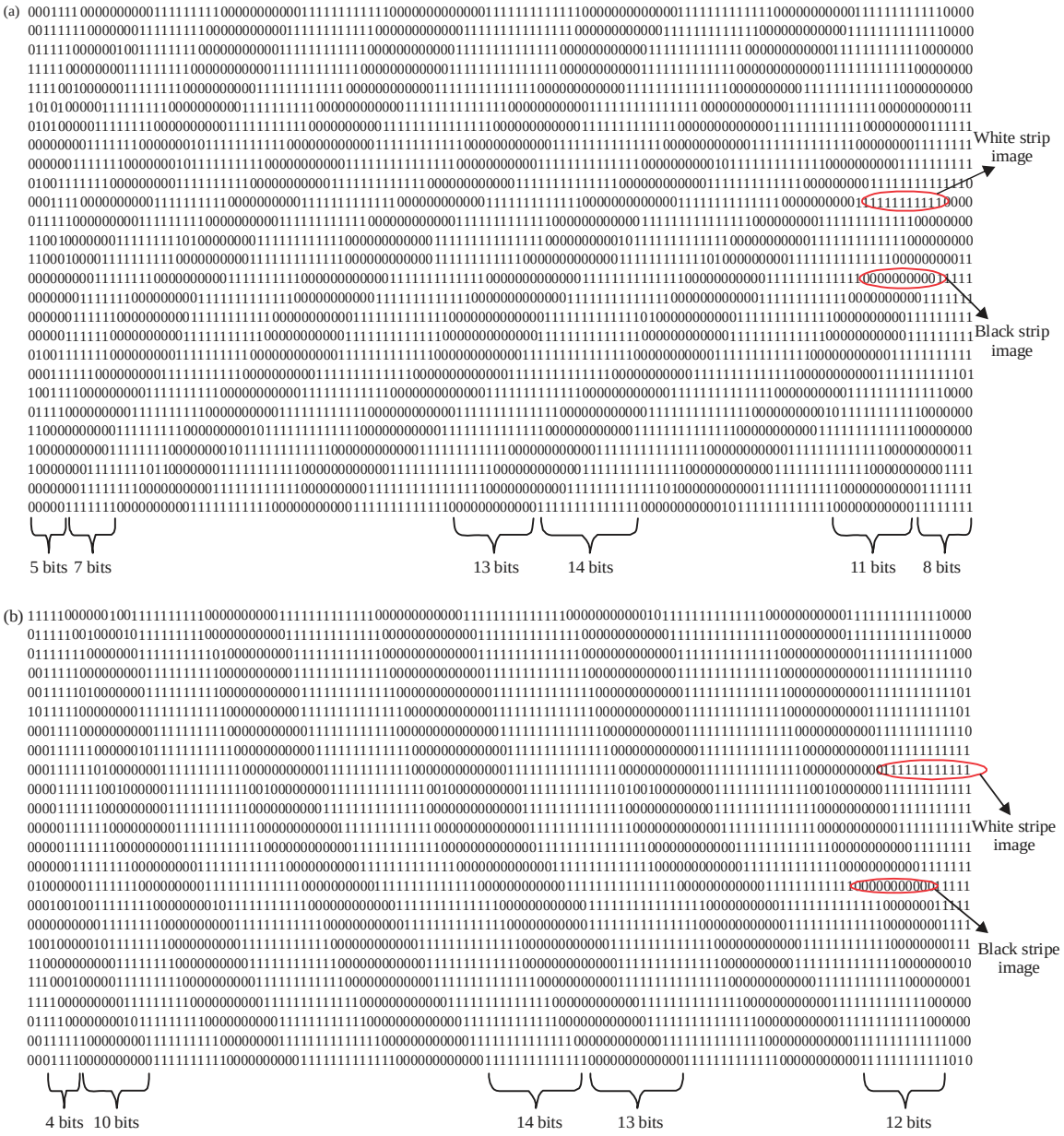

Fig. 13(a-b): (a) Pattern of stripes image while moving in x direction and (b) Pattern of stripes image while moving in -x direction

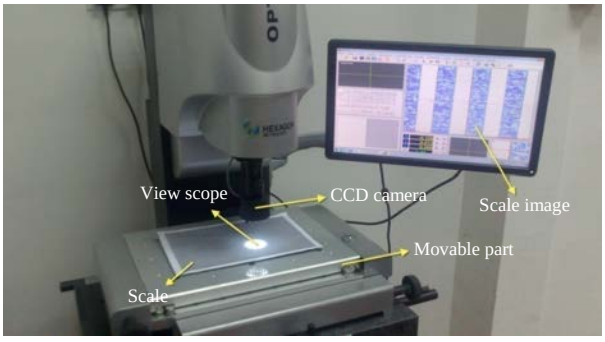

Fig. 14: Optiv light measurement device

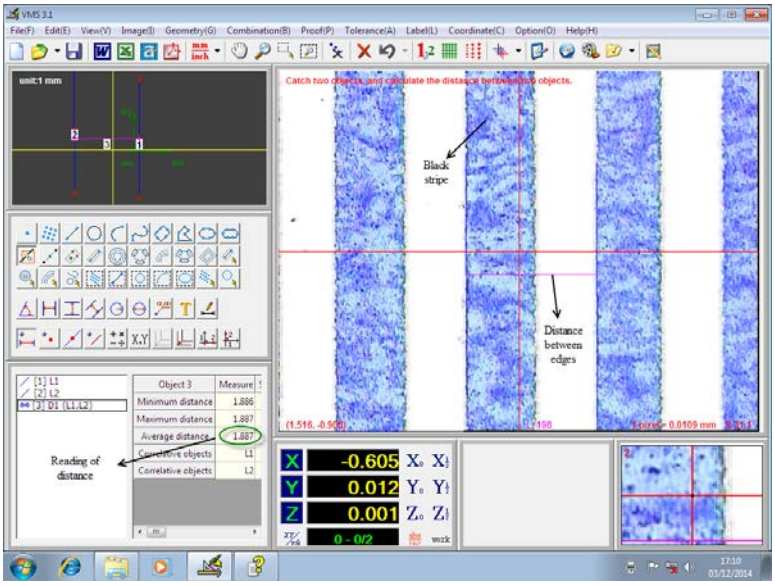

Fig. 15: Measurement of stripes width

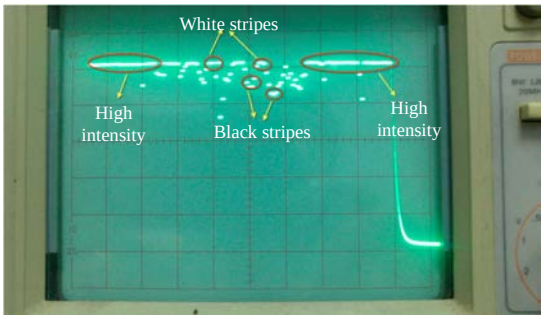

Fig. 16: A 0.5 mm scale stripes image

represented the tracking part. By adjusting the focal length of the CCD camera to 0.7 mm, the image could be seen as shown at a computer screen (Fig. 15). Carefully, two lines were drawn in such a way that the first line was placed on the first edge, while the second line was placed on the next edge. After measurement line button selection, we clicked on the first line and then on the second line that already drew a line between them with the data of distance. Cycle width and grating scale length measurements are shown in Table 1.

Determination of cycle width based on white LEDs: In this section, the measurement of cycle width (two successive stripes) was constructed using the linescan module with built-in white illumination. The cycle width C_W can be found by:

$$C_W = C_f \times P_w \times N_{z+0} \quad (12)$$

Where:

C_f = The crop factor which is defined as the stripes width in the view scope over the sensor array length

Table 1: Reference measurements for transducer evaluation

Grating scale division	Grating scale range (mm)	Average stripe width (mm)
Optiv light device measurement		
0.5	262.095	0.554
	242.543	1.027
1	375.001	1.0075
	565.311	1.007
2	260.354	2.083
	394.109	2.275
	571.214	2.275

P_w = The pixel width

N_{z+o} = The number of zeros and ones for one cycle

As mentioned, the pixel width was 63.5 μm and sensor array length was 8 mm. The linescan module captured three different scale divisions and the result was as follows:

- **0.5 mm:** The image of the stripes in the view scope for 0.5 mm scale is shown in Fig. 16. The convergence of LEDs light was concentrated at the middle of the image, hence the transitions between the stripes were clear. However, the reflected illumination from the black stripes to the linescan chip was high, especially at the boundaries due to the short distance between the lens and the grating scale. Based on the rising and falling edges in the digital image, there are 11 stripes (6.5 cycle) in the view scope, which have length of 6.94 mm (1.108×6.5). However, the middle cycle (reference cycle) in the view scope was captured by 14 pixels in sensor pixels array. The width of this cycle can be calculated by Eq. 15, which is equal 0.667 mm. If the reference cycle width was 1.108 mm, the error in measurement was 38.89%, so it is not recommended to use 0.5 mm scale for displacement tracking because of its high error

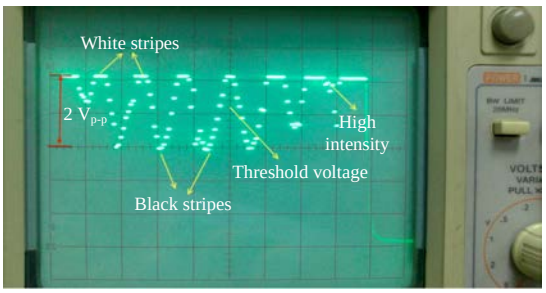

Fig. 17: Stripes image for 1 mm division

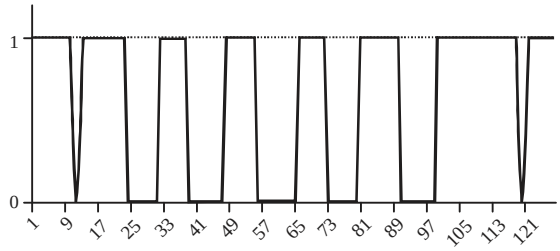

Fig. 18: Stripes image after thresholding process

- **1 mm:** For 1 mm scale, the cycle width was 2.054 mm and overall grating scale length was 242 based on OLM device measurements. The stripes image of 1 mm grating scale is shown in Fig. 17. The transitions between stripes was more clear than the image of 0.5 mm scale and the negative effect of illumination convergence had less effect on the black stripes at the boundaries. The amount of the reflected light from the black stripes at the boundaries was high, while less at the middle of the image. The property of sine wave signal was used to derive the threshold voltage as the same value of the Root Mean Square (RMS) of sine wave signal

The threshold voltage was derived depending upon peak to peak voltage. The signal swings around the value of 4 volts, which has a maximum peak at 5 volts and zero voltage at 4 volts. The equivalent voltage for the signal is:

$$V_{eq} = \frac{V_{max} - V_{zero}}{\sqrt{2}} \quad (13)$$

From the equation, the equivalent voltage is 0.707 V; however, threshold voltage (V_{th}) is derived as:

$$V_{th} = V_{max} - V_{eq} \quad (14)$$

Where, V_{max} is 5 volts, the threshold voltage is 4.29 volts as shown in the Fig. 17. Figure 18 shows the image after thresholding process based on 4.29 volts as threshold voltage. There are 15 stripes (7.5 cycle) which have length of 15.405 mm (7.5×2.054) in the view scope. The middle cycle

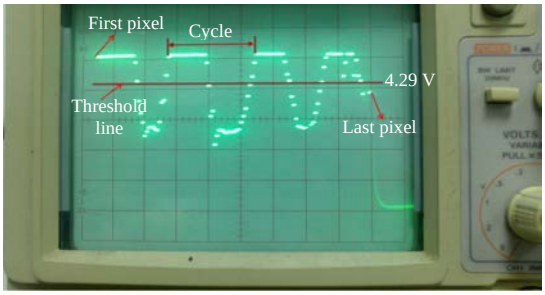

Fig. 19: A 2 mm scale stripes image

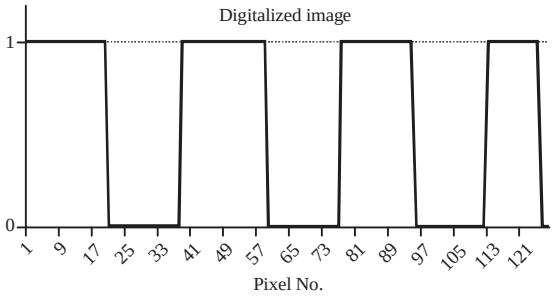

Fig. 20: Stripes image after thresholding process

was captured by 17 pixels and it has width of. The error of cycle width measurement is 1.16% compared to the measurement of OLM device (2.054 mm), therefore the scale of 1 mm can be used for displacement tracking due to low error.

- **2 mm:** For 2 mm scale, the average cycle width were 4.167 mm and 260.354 mm for scale overall length. At the origin, the scale was being captured by linescan module as shown in Fig. 19. The stripes image was clearer than the previous two samples, especially at the boundaries, which increased the capacity of choosing clear stripes in the view scope, as well as the detection of stripes was better. In the view scope, there were 3.5 cycles having width of 14.585 mm (3.5×4.167). Based on Fig. 19, the threshold voltage was selected as the same value (4.29 volts) and the image after thresholding process is shown in Fig. 20. There were 36 pixels capture the middle cycle in the view scope, so the cycle width can be given by:

$$\frac{14.585}{8} \times 36 \times 0.0635 = 4.168 \text{ mm} \quad (15)$$

Hence, the error of cycle width measurement was 0.024% comparing to OLM device measurement (4.167 mm).

Determination of cycle width based on infrared LEDs: In our testing for linescan module, it was important to evaluate

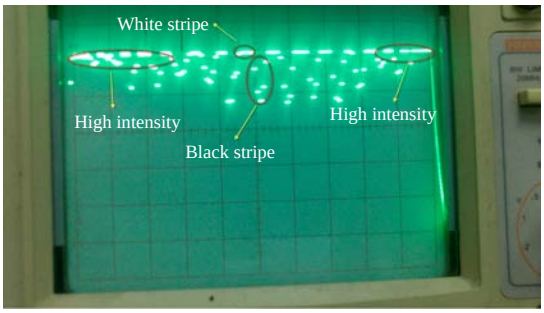

Fig. 21: Stripes image for 0.5 mm scale division

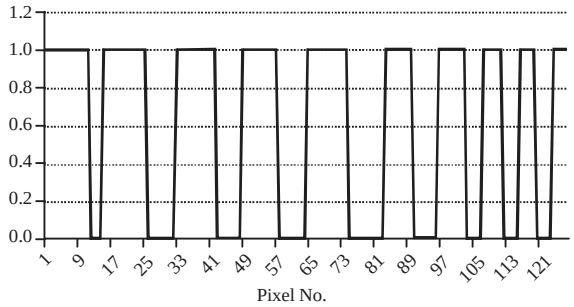

Fig. 22: Stripes image after thresholding process

the performance of the module within invisible light. Infrared LEDs had an invisible light with wave length of 850 nm. In order to compare the performance of visible and invisible light, a plate included, six infrared LEDs was fabricated in arrangement of a ring shape. In that, the average of LED angle is around 49°. The experiments progress can be described based on scale division as follow:

- **0.5 mm:** Starting with 0.5 mm stripe width, the printed grating scale was measured by an OLM device. The average cycle width was 1.108 mm and the overall average scale width was 262.095 mm. The stripes image on the oscilloscope was displayed in Fig. 21. As seen in the figure, the deformation had a significant effect on the stripes but had fewer losses than white LEDs effect. Since the light intensity of infrared LEDs is lower than white LEDs, the stripes image was clearer. The zero voltage of the black stripes is varied, therefore the threshold was selected based on the maximum voltage (5 volts). The stripes image after thresholding process is shown in Fig. 22. There are 19 stripes (9.5 cycles) in the view scope, which have length of 10.526 mm. However, 17 pixels captured the cycle at the middle and the width of this cycle was 1.42 mm. The error of the measurement was high (28.2%) comparing to OLM device measurement (1.108 mm). Thus, 0.5 scale is not qualified for displacement measurements

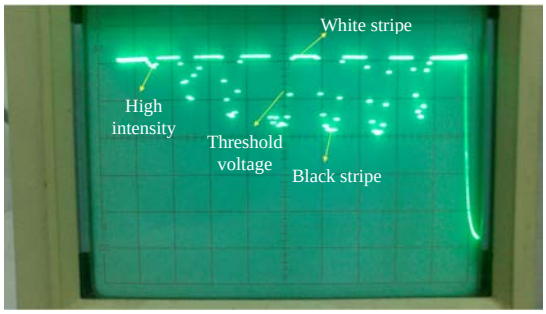

Fig. 23: Stripes image of 1 mm scale

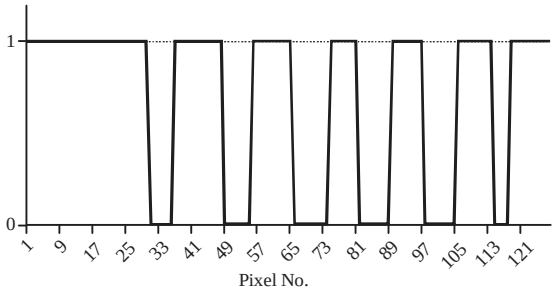

Fig. 24: A 1 mm scale image after thresholding process

- **1 mm:** By scanning the scale at reference position, the image captured is shown in Fig. 23. Comparing this image with the image based on white LEDs, using infrared LEDs provided more clearness especially for black stripes. In microcontroller, the image was converted to a digital image based on 4.29 volts as the threshold voltage as shown in Fig. 24. In the view scope, there are 6.5 cycles, which have length of 13.351 mm (6.5×2.054). The cycle at the middle which is targeted for displacement tracking was captured by 19 pixels and its width was 2.013 mm and the width measurement error was 1.97% comparing to OLM device measurement
- **2 mm:** At starting time, the image on the oscilloscope display screen is shown in the figure below (Fig. 25). As seen, the clearance at the black stripes was high compared with white LEDs and its pixels were closed to each other due to low reflected light. Based on threshold line value, the stripes image could be digitalized to binary values zero or one as illustrated in Fig. 26. In addition, the slope of edges was sharp and the pixels of black stripes were closed to each other compared with other scales. There were fourth cycles in the view scope, which had length of 16.668 mm. However, 32 pixels captured the cycle at the middle of the scope and it had width of 4.101 mm. The measurement error was 1.58% comparing to OLM measurement (4.167 mm)

Table 2: Main parameters of the experiments

	Sheet type					
	A4		A3		A2	
Grating scale division	2 mm	1 mm	2 mm	1 mm	2 mm	1 mm
Reference sheet length (mm)	260.354	242.543	394.109	375.001	571.214	565.311

Table 3: Linescan module displacement measurements

	Linescan module measurements					
Grating scale division	1 mm			2 mm		
White LEDs						
Reference range (mm)	242.543	375.001	565.311	260.354	394.109	571.214
Average displacement (mm)	238.06	365.39	555.95	259.84	389.69	563.18
Average error (%)	1.85	2.56	1.66	0.20	1.12	1.41
Standard deviation (mm)	4.91	14.61	12.89	6.13	17.59	12.47
Infrared LEDs						
Reference range (mm)	242.543	375.001	565.311	260.354	394.109	571.214
Average displacement (mm)	239.19	367.8	558.5	260.32	391.08	566.06
Average error (%)	1.38	1.92	1.21	0.014	0.77	0.90
Standard deviation (mm)	5	2.93	12.47	7.81	10.86	11.63

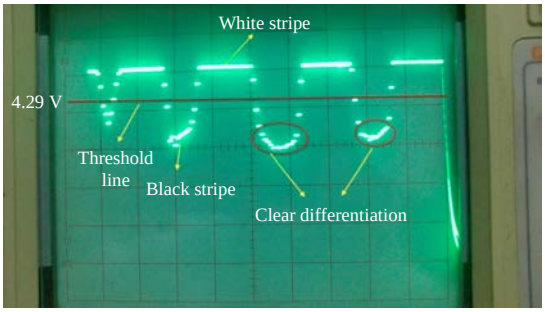

Fig. 25: A 2 mm stripes image

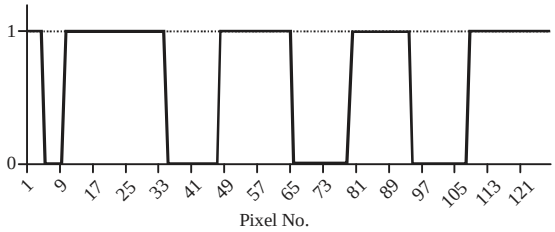

Fig. 26: Binary values based on thresholding process

DISCUSSION

Displacement measurements over different ranges: The range of travelling did not affect the errors significantly if and only if the linescan module had capability of cycles counting at all positions on the grating. Three sets of grating scales were designed and printed over A2, A3 and A4 paper sizes. Every set had two scale divisions (1 and 2 mm). Firstly, the grating scale length was measured by using OLM device and these measurement was represented as the reference values for our linescan module measurements. The main parameters of the sets is shown in Table 2.

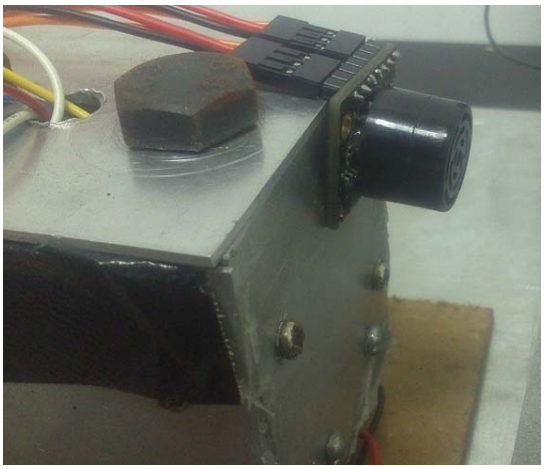

Fig. 27: Ultrasonic sensor as seen on the transducer

Based on the measurements in above table, the linescan displacement measurements were evaluated. Every grating scale was scanned from the beginning to the end by linescan module 30 times. The average displacement measurement, average error and deviation of measurements were recorded in Table 3. As seen in the below table, the scales 1 and 2 mm were qualified to be used in displacement measurements for short and long range measurements. The lower errors were yield with infrared LED and using 2 mm grating scale.

Displacement measurements based on the integration of linescan module and ultrasonic sensor: In our study for linescan sensor to measure the displacement, the initial position for measurement was 0 mm. Now, the scenario of initial position was critical when the start point was not 0 mm. At X mm on the slider, the recorded displacement by the linescan module was 0 mm. Therefore, uncorrected

measurement was being recorded. By installing an ultrasonic sensor on the transducer, the first position could be provided for linescan module. Figure 27 shows the installation of ultrasonic sensor on the transducer. The ultrasonic sensor provided the displacement in proximity. Moreover, an absolute value could be recorded using it in term of displacement.

At first, the test was prepared for ultrasonic sensor, it had a range detection of 4000 mm and resolution of 5 mm. Table 4 has the recorded displacements based on an ultrasonic sensor. The average error was -2.19%, while a 6.86% as the average deviation. From that, it can be noticed that there was high error of data compared with linescan module and OLM device measurements.

After adding the sonic sensor to the module, the displacement was recorded at several points at the scale. The initial displacement reading was gotten from the ultrasonic sensor and then manual movement was applied to the module over 1000 mm. This movement took several times and every time the measurement was generated from the initial reading plus the overall reading of module measurement. Grating scale with division of 2 mm and infrared LEDs were used in this experiment. Over 1000 mm range, Table 5 contains the displacement measurements based on sensors integration. The errors based on sensors integration were increased by 0.62% in comparison with linescan average error, which was based on infrared LEDs and 2 mm scale. The regression line for sensors integration measurements illustrates the linearity of the data which has square roots of 0.999 (Fig. 28). In contrast, it was decreased by 1.95% compared with the ultrasonic sensor measurements. The increase in errors was generated from the initial position that was observed from the sonic sensor.

Table 4: Displacement measurements based on ultrasonic sensor

Measured displacement (mm)	Actual distance (mm)	Error (%)
155	150	3.33
210	200	5
258	250	3.2
290	300	-3.33
357	350	2
513	500	2.6
615	600	2.5

Comparison our transducer against previous transducers in linear displacement measurements: The measurement of displacement is a very important issue encompassing a large number of optical solutions. A brief overview of some optical methods is presented to be compared with our transducer in linear displacement measurements. Table 6 summarizes the characteristics of the different optical methods of

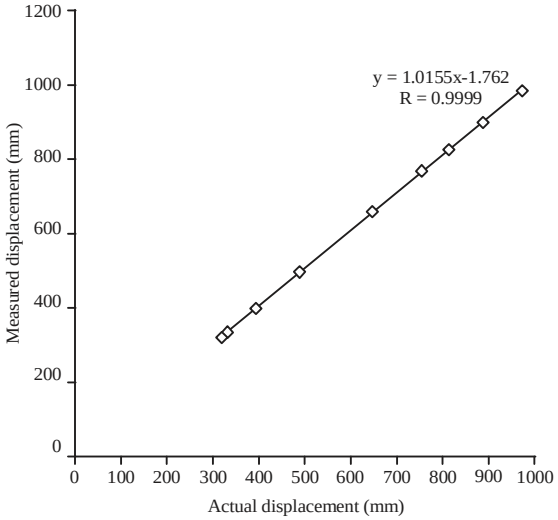

Fig. 28: Regression line for the sensors integration measurements

Table 5: Linescan module and ultrasonic sensor integration results over a range of 1000 mm

Measured displacement (mm)	Initial position (mm)	Actual displacement (mm)	Error (%)	Standard deviation (mm)
318.16	85	317.16	0.31	0.71
333.16	100	331.16	0.60	1.41
398.16	165	393.16	1.26	3.54
494.2	265	488.2	1.21	4.24
657.18	420	646.18	1.67	7.78
767.24	530	753.24	1.82	11.90
825.12	600	813.12	1.45	10.49
898.22	665	888.22	1.11	11.07
983.16	750	973.16	1.02	12.87
1159.2	930	1143.2	1.38	14.31
Average (%)			1.18	7.83

Table 6: Performance of different optical methods for displacement measurements

Transducer	Method	Range	Resolution	Accuracy
Our proposed transducer	Pixel shifting method	1000 mm	63.5 μm	0.01%
Optical potentiometer (Lang *et al*., 1992)	Beer's Law	940 mm	10 mm	0.01%
Optical lever (Liu *et al*., 2006)	Plane mirrors	850 nm	4 nm	10 nm
PSD (Miranda *et al*., 2014)	Resistive charge division	100 mm	72 μm	500 μm
Photoelectric incremental encoder (Israel *et al*., 2003)	Direct traceability	270 mm	27 nm	2 μm
Optical encoder (Kao and Lu, 2005)	Fractional talbot effect	600 mm	0.1 μm	0.2 μm

displacement solutions. The optical potentiometer provided a large travelling range and a high accuracy, however the resolution was larger than our proposed transducer by 8 mm. In using of optical lever sensor, the measurement range was too low, therefore this type of optical sensors cannot be used for large range of measurement. In case of optical encoder, the resolution and accuracy were high, however the Talbot method is a complicated approach when it comes to industrial applications. In this study, the cost of linescan sensor is low comparing with position sensor detector. The proposed transducer in this study provides measurement for large traveling range (1000 mm), high resolution (2 mm) and low errors (1.18%).

CONCLUSION

A linear motion transducer was designed and fabricated which encoded position directly from the image of the grating scale and measured the displacement based on pixel differential method. The output of the linescan sensor was a periodic signal that had the image of the stripes pattern. The white stripe and black stripe interpolated high voltage and low voltage respectively, because of the sensitivity of the sensor to the reflected light from the grating scale. The illumination system had six LEDs of infrared and white lights, which were arranged in a ring shape. The analogue signal of the sensor was digitalized based on threshold value to observe pure binary signal. While the sensor was sensitive to the light, the light source with high wavelength (infrared LEDs) provided clearer patterns than the visible light (white LEDs). The result was a precise and cost effective displacement transducer. The stripes image of 2 mm scale division was clearer than 1 and 0.5 mm scale divisions due to light convergence. The linescan module had low error and low deviation, if the grating scale division was 2 mm and the used illumination was infrared LEDs. In this case, the average error was 0.9% and the standard deviation was 11.63 mm over travelling range up to 500 mm. However, if the measurement did not start at the beginning of the scale, the initial position was missed. So, an ultrasonic sensor was added to the transducer so as to provide the initial position measurement. The integration of two sensors could measure ranges up to 1 m with average error of 1.18% and standard deviation of 7.83 mm.

REFERENCES

Alsayed, A. and M.R. Mahadi, 2014. Precise positioning based on pixel differential in linear optical sensor array. Agric. Agric. Sci. Procedia, 2: 10-17.

Cano-Garcia, A., J.L. Lazaro and P.R. Fernandez, 2007. Simplified method for radiometric calibration of an array camera. Proceedings of the IEEE International Symposium on Intelligent Signal Processing, October 3-5, 2007, Alcala de Henares, pp: 1-5.

Corradi, P., L. Ascari, A. Menciassi and C. Laschi, 2008. A micro-optical transducer for sensing applications. Int. J. Optomechatronics, 2: 361-381.

Feng, M.Q., 1996. An experimental study of an electro-optical displacement sensor. Nondestructive Testing Evaluat., 13: 5-14.

Giniotis, V. and K.T.V. Grattan, 2002. Optical method for the calibration of raster scales. Measurement, 32: 23-29.

Gou, Y., Y. Xuan, Y. Han and Q. Li, 2011. Enhancement of light-emitting efficiency using combined plasmonic Ag grating and dielectric grating. J. Luminescence, 131: 2382-2386.

Haus, J., 2010. Optical Sensors: Basics and Applications. John Wiley and Sons, New York, ISBN: 9783527629442, Pages: 128.

Israel, W., I. Tiemann, G. Metz, Y. Yamaryo, F. Maeda and T. Shimomura, 2003. An international length comparison at an industrial level using a photoelectric incremental encoder as transfer standard. Precis. Eng., 27: 151-156.

Kajima, M. and K. Minoshima, 2014. Calibration of linear encoders with sub-nanometer uncertainty using an optical-zooming laser interferometer. Precision Eng., 38: 769-774.

Kao, C.F. and M.H. Lu, 2005. Optical encoder based on the fractional Talbot effect. Opt. Commun., 250: 16-23.

Lambert, A.J., E.M. Daly, E. Delestrange and J.C. Dainty, 2011. Supplementary active optics for illumination within an adaptive optics system. J. Mod. Optics, 58: 1716-1728.

Lang, S.R., D.J. Ryan and J.P. Bobis, 1992. Position sensing using an optical potentiometer. IEEE Trans. Instrum. Meas., 41: 902-905.

Lee, C.Y. and J.L. Liu, 2012. Illumination based on high-power white light-emitting diode array. Int. J. Green Energy, 9: 421-429.

Liu, X., Y. Wu, Y. Zhang and G. Yang, 2006. Optical measurement technology of nano-scale displacement. Proceedings of the International Technology and Innovation Conference, November 6-7, 2006, Hangzhou, China, pp: 343-348.

Mahadi, M.R., 2011. Critical issues in precise machining of oversize moulds in polystyrene. Ph.D. Thesis, University of Southern Queensland, Toowoomba, Queensland.

Miranda, P.A., U. Wahl, N. Catarino, M.R. da Silva and E. Alves, 2014. Performance of resistive-charge position sensitive detectors for RBS/Channeling applications. Nuclear Instrum. Methods Phys. Res. Sect. A: Acceler. Spectrom. Detect. Assoc. Equip., 760: 98-106.

Miwa, M., M. Ishii, Y. Koike and M. Sato, 2000. Screen projection camera for ranging far away objects. Proceedings of the 15th International Conference on Pattern Recognition, Volume 4, September 3-7, 2000, Barcelona, pp: 744-747.

Nagai, I., G. Yamauchi, K. Nagatani, K. Watanabe and K. Yoshida, 2013. Positioning device for outdoor mobile robots using optical sensors and lasers. Adv. Robotics, 27: 1147-1160.

Protzman, J.B. and K.W. Houser, 2006. LEDs for general illumination: The state of the science. Leukos, 3: 121-142.

Richard, H., 2007. Illumination Optics. In: Encyclopedia of Optical Engineering, Driggers, R.G. (Ed.). Marcel Dekker, New York, pp: 760-772.

Shi, S., Y. Cao, Y. Xiao and Y. Wu, 2014. A study of the impact on telecentricity to the illumination system based on CCD imaging. Optik-Int. J. Light Electron Optics, 125: 5853-5860.

Viollet, S. and N. Franceschini, 2010. A hyperacute optical position sensor based on biomimetic retinal micro-scanning. Sensors Actuators A: Phys., 160: 60-68.

Zhu, Z.M., X.H. Qu, G.X. Jia and J.F. Ouyang, 2011. Uniform illumination design by configuration of LED array and diffuse reflection surface for color vision application. J. Display Technol., 7: 84-89.